Mechanisms of Northern Tropical Atlantic variability and response to CO_2 doubling

Wim-Paul Breugem, Wilco Hazeleger & Reindert J. Haarsma

Royal Netherlands Meteorological Institute (KNMI)

De Bilt, Netherlands

phone: +31-30-2206700; fax: +31-30-2202570; e-mail: breugem@knmi.nl

ABSTRACT

A model study has been made of the mechanisms of the meridional mode in the Northern Tropical Atlantic (NTA) and the response to a doubling of atmospheric CO_2. The numerical model consists of an atmospheric General Circulation Model (GCM) coupled to a passive mixed-layer model for the ocean. Results from two simulations are shown: a control run with present-day atmospheric CO_2 and a run with a doubled CO_2 concentration. The results from the control run show that the Wind-Evaporation-SST (WES) feedback is confined to the deep NTA. Furthermore, the temporal evolution of the meridional mode is phase-locked with the seasonal cycle of the climatological Intertropical Convergence Zone (cITCZ). The WES feedback is positive in boreal winter and spring when the cITCZ is located close to the equator, but negative in summer and fall when the cITCZ shifts towards the north of the deep NTA. Similarly, damping of the SST anomalies in the deep NTA by moisture-induced evaporation anomalies is much stronger in summer and fall than in winter and spring, related to a change in anomalous moisture transport. The results from the double-CO_2 run show a substantial northward shift of the cITCZ in boreal winter and spring, but little change in summer and fall. The change in the cITCZ can be explained by strong warming at the high northern latitudes and a seasonally dependent WES feedback and accompanying changes in moisture transport in the deep NTA. The latter indicates that the change in the cITCZ is subject to phase-locking with the seasonal cycle of the cITCZ itself. The meridional mode in the double-CO_2 run weakens by 10-20 %. This originates from the weakening of the positive WES feedback in the deep NTA, which in turn is attributed to the northward shift of the cITCZ: because in the double-CO_2 run the cITCZ stays less long south of the deep NTA, the positive WES feedback in the deep NTA acts less long, and damping by moisture-induced evaporation anomalies starts earlier than in the control run.

1 Introduction

Increasing evidence suggests that the warming of the earth's climate since the nineteenth century is caused by an enhanced greenhouse effect from higher concentrations of greenhouse gases in the atmosphere (IPCC 2001). Of all greenhouse gases, the increase in the atmospheric concentration of carbon dioxide (CO_2) over the past 150 years has been responsible for the strongest radiative forcing. The warming of the earth's climate will likely also affect the dominant patterns of climate variability. This paper is concerned with the effect of increasing atmospheric CO_2 on climate variability in the tropical Atlantic.

On interannual time scales, tropical Atlantic climate variability is dominated by a zonal mode and a meridional mode (Carton et al. 1996, Ruiz-Barradas et al. 2000, Xie and Carton 2004). The zonal mode is similar to El Niño–Southern Oscillation (ENSO) in the Pacific (Zebiak 1993). It is characterized by anomalous Sea Surface Temperatures (SSTs) centered slightly south of the eastern equatorial Atlantic, zonal wind anomalies directed along the equator, variations

in the equatorial thermocline depth, and a displaced Intertropical Convergence Zone (ITCZ) in the eastern equatorial Atlantic. In this study we consider only the meridional mode. This mode is characterized by variations in SSTs in the Northern Tropical Atlantic (NTA) on the order of 0.5 °C, changes in the strength of the northeasterly trade winds, and cross-equatorial surface wind anomalies pointing towards (away from) the anomalously high (low) SSTs. The cross-equatorial wind anomalies displace the ITCZ in the western tropical Atlantic, which has a pronounced influence on rainfall in northeast Brazil (Moura and Shukla 1981) and to less extent the African Sahel (Folland et al. 1986).

The origin of the meridional mode has been investigated in numerous studies over the past decades, see the reviews by Marshall et al. (2001) and Xie and Carton (2004). Interannual variations in the northeasterly trade winds in boreal winter are the imprint of both ENSO and North Atlantic Oscillation (NAO) events on the NTA (Nobre and Shukla 1996, Sutton et al. 2000, Czaja et al. 2002). Changes in the strength of the trade winds cause changes in wind-induced latent cooling of the ocean and thus generate SST anomalies (Carton et al. 1996). Hydrostatic pressure adjustment to the SST anomalies gives rise to sea-level pressure anomalies, which in turn force cross-equatorial wind anomalies (Moura and Shukla 1981, Lindzen and Nigam 1987). The cross-equatorial wind anomalies further change wind-induced latent cooling and act to amplify the SST and pressure anomalies. Elements of this positive feedback have already been analyzed by Hastenrath (1984). Xie and Philander (1994) proposed a similar feedback mechanism to explain why the Pacific ITCZ is locked to the northern hemisphere. The study by Chang et al. (1997) suggested that this feedback mechanism may be an important contributing factor to coupled decadal variability in the tropical Atlantic. Xie (1999) called it the Wind-Evaporation-SST (WES) mechanism. It is still under debate whether the SST anomalies in the NTA are primarily the result of external forcing by ENSO and NAO or originate mainly from a local WES feedback. Increasing evidence suggests that the WES feedback is confined to the deep NTA, while the external forcing dominates further to the north of the NTA (Chang et al. 2000, Chang et al. 2001, Czaja et al. 2002, Kushnir et al. 2002, Frankignoul and Kestenare 2005).

Ocean dynamics seem to play a minor role for NTA variability. There is some evidence of anomalous heat transport by the mean meridional current, which tends to damp the SST anomalies in the deep NTA and partly counterbalances the positive WES feedback acting in the same region (Xie 1999, Seager et al. 2001, Chang et al. 2001).

The development of the meridional mode displays a seasonal cycle (Czaja et al. 2002, Chiang et al. 2002). The SST anomalies are initiated by trade wind anomalies in boreal winter, when ENSO and NAO events are strongest. These trade wind anomalies persist till spring and consequently the SST anomalies reach their maximum in the same season. In summer and fall the SST anomalies are damped by anomalies in the latent heat flux related to thermodynamic adjustment of the atmosphere to the SST anomalies. Czaja (2004) claimed that the seasonal cycle of SST anomalies in the NTA can be primarily explained by the seasonal dependence in the remote forcing by ENSO and NAO. The present study indicates that in the deep NTA the seasonal cycle of SST anomalies also depends on a seasonally dependent WES feedback and associated changes in moisture transport, which in turn are regulated by the seasonality of the climatological ITCZ.

The main aim of this study is to gain further insight in the structure and mechanisms of the meridional mode and the sensitivity to a doubling of atmospheric CO_2. The focus is on the local air-sea interactions and their seasonal dependence. To this purpose two simulations have been performed with a General Circulation Model (GCM) coupled to a passive mixed-layer model for the ocean, where we only varied the CO_2 concentration. The model is described in more detail in section 2. The results for the change in the tropical Atlantic climatology are presented in section 3 and for the change in the tropical Atlantic variability in section 4. In section 5 the

results are discussed. Finally, in section 6 the main results and conclusions are summarized.

2   Model

The model used for the simulations consists of an Atmospheric General Circulation Model (AGCM), a land bucket model, and a passive mixed-layer model for the ocean. This model configuration has been used before by Haarsma et al. (2005) and Hazeleger et al. (2005). The AGCM, nicknamed SPEEDY, is a spectral primitive equations model with a horizonal Gaussian grid and triangular truncation at wavenumber 30, 7 layers in the vertical, a time step of 30 minutes, and simplified physical parameterizations. Compared to state-of-the-art AGCMs it is an order-of-magnitude faster, but it has still reasonable accuracy. A five-layer version of this model was described and validated in detail by Molteni (2003). The seven-layer version used in the present study contains some modifications made to the original model, the most important the parameterization of cloud cover. To accommodate climate change experiments, the absorptivity parameter for long-wave radiation in the CO_2 band is parameterized as function of the CO_2 concentration. More details on the modifications can be found in Hazeleger et al. (2003), where also a description is given of the land bucket model.

The passive mixed-layer model for the ocean is described by Haarsma et al. (2005). The daily-mean temperature of the mixed layer is calculated from:

$$\frac{\partial T}{\partial t} = \frac{Q}{h\rho_w c_p} + F_{\text{clim}}, \tag{1}$$

where Q is the daily-mean net surface heat flux into the ocean, h is the time-independent mixed-layer depth, ρ_w is the density of seawater, c_p is the specific heat capacity of seawater, and F_{clim} represents basically the climatological ocean heat flux and is prescribed. The evolution of sea ice is computed from a thermodynamic ice model. The same horizontal grid is used in the ocean model as for the atmosphere in SPEEDY, and the time step is one day.

The prescribed ocean heat transport (F_{clim}) in equation (1) has been computed from a separate model run of 200 years with the ocean module replaced by observed climatological SSTs, according to:

$$F_{\text{clim}} = \frac{\partial T_{\text{clim}}}{\partial t} - \frac{Q_{\text{diag}}}{h\rho_w c_p}, \tag{2}$$

where Q_{diag} is the surface heat flux diagnosed from the simulation.

The passive mixed-layer model for the ocean is basically a thermodynamic model, where ocean dynamics are only implicitly incorporated in F_{clim}. SST anomalies arise only from interactions with the atmosphere. This is a suitable model for studying the meridional mode in the tropical Atlantic, for which ocean dynamics play a minor role. Other climate variability phenomena for which ocean dynamics are important, such as ENSO and the zonal mode in the Atlantic, are not simulated by this model. As discussed in the previous section, the external forcing of the meridional mode originates partly from ENSO. The fact that ENSO is not captured by our model implies that the strength of the external forcing will be weaker compared to models that do account for ENSO. The focus of the present study is however not on the teleconnection with ENSO, but on the local air-sea interactions in the tropical Atlantic itself.

Results from two model runs will be shown. In the control run, case 1C, the atmospheric CO_2-concentration is equal to 342.5 ppmv, which is the averaged concentration over roughly the past fifty years. In the second run, case 2C, the atmospheric CO_2-concentration is twice as large (685 ppmv), which is in the range of 490-1260 ppmv projected by carbon cycle models for the year 2100 (IPCC 2001). The prescribed ocean heat transport (F_{clim}) in equation (1) is
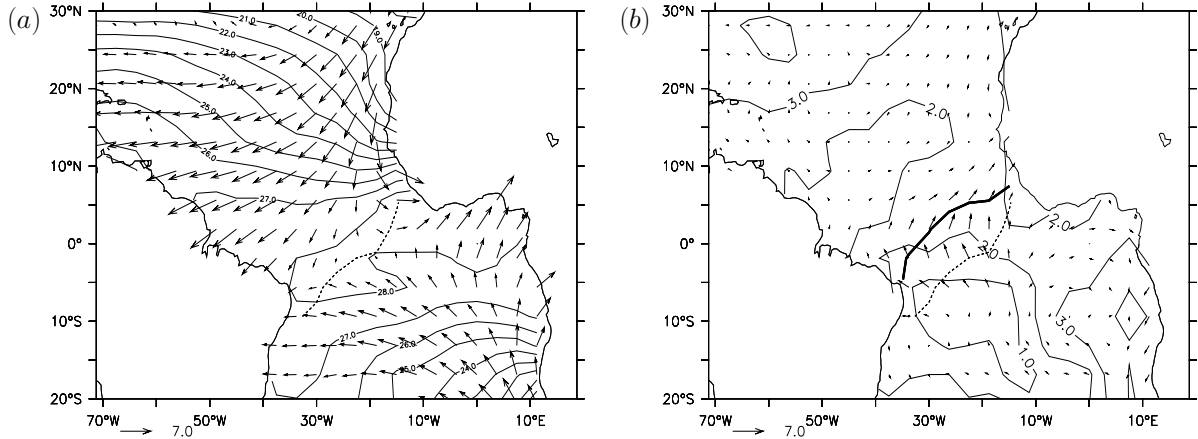
Figure 1: Climatological SSTs (thin contours, in °C) and near-surface winds (vectors, in m/s) for April, along with the location of the marine ITCZ (dashed line for case 1C, thick solid line for case 2C). (a) Case 1C. (b) Change in case 2C relative to case 1C.

kept the same as in the control run, based on the assumption that changes in F_{clim} will have little influence on the meridional mode in the tropical Atlantic. The simulations were run for 260 years. Only the last 200 years were used in our analysis, and linear trends over this period were removed from the data. The climate sensitivity, defined as the increase in global mean near-surface air temperature after a doubling of the atmospheric CO_2 concentration, is equal to 5.5 °C. This is larger than the range of 3.5 ± 0.9 °C projected by coupled GCMs (IPCC 2001), which is possibly due to the fixed ocean heat transport in our simulations.

3   Changes in tropical Atlantic climatology

This section presents the results for the changes in tropical Atlantic climatology in case 2C with respect to case 1C. Figure 1 depicts the climatological SSTs, near-surface winds and the marine ITCZ for April. The ITCZ is defined here as the zone where the meridional near-surface wind is closest or equal to zero. In case 1C the marine ITCZ is located too far to the south in the western part of the Atlantic basin compared to observations (e.g. Xie & Carton 2004), which is a well-known artifact of many GCMs (Biasutti et al. 2006). Also the magnitude of the near-surface winds is smaller than in the observations, but SSTs are well simulated, inherent to the prescribed ocean heat transport in our simulations. In case 2C SSTs have increased over the whole tropical Atlantic, with SSTs exceeding 31°C at the east and southeast of the equator. The marine ITCZ has shifted to the north over the entire basin width, with the shift amounting almost 10° near 30°W. Changes in near-surface winds are strongest in the deep tropics and predominantly meridional. The C-shaped change in the near-surface wind pattern near the equator is accompanied by an increase in the northward SST gradient (figure 1.b).

Figure 1 shows that the SSTs and winds in the NTA are fairly zonally homogeneous, and as a first approximation they may therefore be represented by their zonal averages. To explore the changes in the seasonal cycle of the tropical Atlantic climate, the SSTs and winds have been zonally averaged over the Atlantic from 55-20°W and plotted in figure 2 as function of time. The increase in SSTs in case 2C relative to case 1C is similar for each month. SSTs in case 2C exceed 30°C and are centered around the marine ITCZ in the period August-October. The marine ITCZ has shifted substantially to the north in boreal winter and especially spring, when it amounts roughly 5° on zonal average, but the displacement is small in summer and marginal
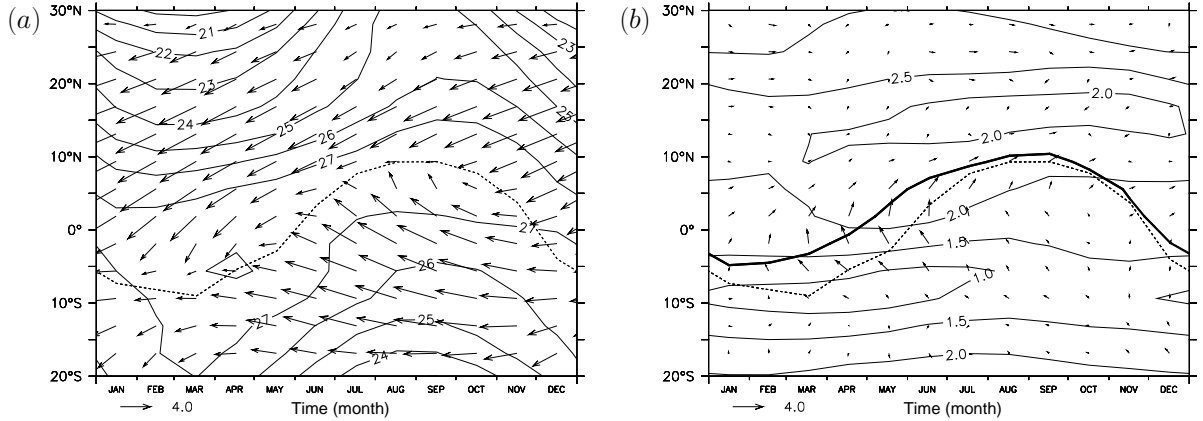
Figure 2: Time-latitude graph of climatological SST (thin contours, in °C) and near-surface winds (vectors, in m/s), both zonally averaged over the Atlantic from 55-20°W, along with the location of the marine ITCZ (dashed line for case 1C, thick solid line for case 2C). (a) Case 1C. (b) Change in case 2C relative to case 1C.

in fall.

The northward shift of the ITCZ in figures 1.b and 2.b is accompanied by a C-shaped change in the near-surface wind field in combination with an increase in the northward SST gradient near the equator. This suggests that the shift of the ITCZ results from a positive WES feedback (Hastenrath 1984, Carton et al. 1996, Chang et al. 1997, Xie 1999). A similar mechanism was mentioned before by Xie and Philander (1994) to explain why the Pacific ITCZ is locked to the northern hemisphere, and by Chiang and Bitz (2005) and Broccoli et al. (2006) to explain that an interhemispheric asymmetry in warming at high latitudes will shift the ITCZ towards the warmer hemisphere. This mechanism has been investigated in more detail for the current simulations and will be discussed below.

Figure 3 presents the change in the latent surface heat flux and the net surface heat flux. Between roughly 10°S and 10°N the change in the latent heat flux resembles the change in the net heat flux. Both fluxes exhibit a skewed dipole pattern centered around the ITCZ of case 2C and in boreal spring their amplitudes are comparable.

The changes in the latent heat flux have been further decomposed into separate contributions from changes in near-surface wind speed, specific humidity and static stability according to respectively:

$$\Delta\overline{LW} = -L_v \left.\overline{\rho_a C}\right|_{1C} \overline{(q_s - q)}_{1C} \left[\left.\overline{\sqrt{u^2 + v^2 + w_*^2}}\right|_{2C} - \left.\overline{\sqrt{u^2 + v^2 + w_*^2}}\right|_{1C} \right] \quad (3)$$

$$\Delta\overline{LQ} = -L_v \left.\overline{\rho_a C}\right|_{1C} \left[\overline{(q_s - q)}_{2C} - \overline{(q_s - q)}_{1C} \right] \left.\overline{\sqrt{u^2 + v^2 + w_*^2}}\right|_{1C} \quad (4)$$

$$\Delta\overline{LS} = -L_v \left[\left.\overline{\rho_a C}\right|_{2C} - \left.\overline{\rho_a C}\right|_{1C} \right] \overline{(q_s - q)}_{1C} \left.\overline{\sqrt{u^2 + v^2 + w_*^2}}\right|_{1C} \quad (5)$$

where the overbar denotes the climatological monthly mean, the subscripts 1C and 2C denote for which model run a term is evaluated, L_v is the latent heat of vaporization of water, ρ_a is the atmospheric air density at near-surface, C is a coefficient dependent of the static stability of the atmospheric boundary layer, q_s and q are the saturation specific humidity at sea surface and the near-surface specific humidity respectively, u and v are the zonal and the meridional near-surface velocity respectively, and w_* is a constant representing the unresolved turbulent
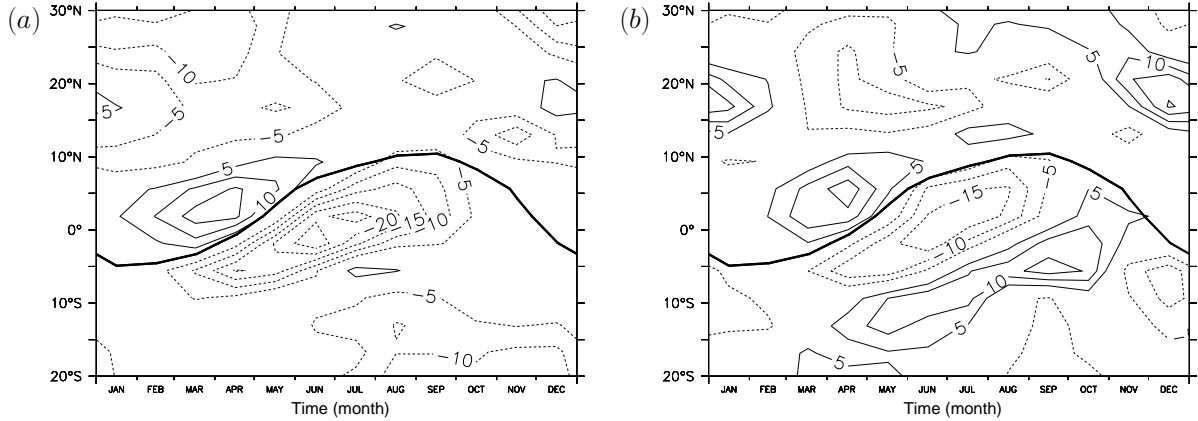
5

Figure 3: Same as figure 2.b, but now thin contours represent the change (in W/m^2) in respectively (a) the downward surface latent heat flux and (b) the net surface heat flux.

wind. The contributions and their sum are shown in figure 4. The sum of the contributions resembles the total latent heat flux quite well, cf. figures 3.a and 4.d.

The dipole in the total latent heat flux is reflected in the contribution from wind speed changes (figure 4.a). The wind speed has decreased north of the ITCZ in winter and spring, while it has become larger south of the ITCZ from March till September, resulting in weaker and stronger latent cooling, respectively. The contribution from the specific humidity difference is negative throughout the year, though significantly weaker north of the ITCZ in spring than south of the ITCZ in summer (figure 4.b). The latter may in part be explained by changes in wind from spring to summer. The spring wind anomalies are responsible for anomalous advection of warm and humid air from the ITCZ towards the north, which results in anomalous moistening of the atmospheric boundary layer and damping of latent cooling. Contrary to spring, the summer wind anomalies are responsible for drying of the atmospheric boundary layer and tend to amplify latent cooling. Changes in subsidence and turbulent intrusion on top of the boundary layer may also have played a role in causing the spring-summer asymmetry in the contribution from the specific humidity difference, but this has not been further explored. The contribution from changes in static stability is shown in figure 4.c. This contribution is positive all year round, indicating that the vertical potential temperature gradient and hence the static stability of the atmospheric boundary layer has increased. This is likely related to the fact that in the tropics the atmospheric lapse rate in the lower troposphere is close to the moist adiabatic lapse rate, set by the temperature and moisture content in the atmospheric boundary layer, which implies that an increase in temperature and moisture content, as in case 2C, will yield a stronger vertical potential temperature gradient (Held & Soden 2006). Notice that the spatial pattern in figure 4.c seems less related to the seasonal cycle of the ITCZ compared to the other two contributions.

From figures 2-4 the following picture emerges. The stronger increase in SSTs north of the ITCZ compared to the SSTs south of it, causes a decrease in the northward pressure gradient owing to hydrostatic adjustment of the pressure to the SST field (Moura and Shukla 1981, Lindzen and Nigam 1987). This forces the C-shaped pattern of near-surface wind field changes directed towards the north and the northward shift of the ITCZ. Consequently, the absolute wind speed becomes smaller north of the ITCZ in spring, while larger south of the ITCZ in summer, resulting in respectively reduced and enhanced latent cooling. The associated changes in moisture transport act to amplify this dipole in the latent heat flux. The latent heat flux dipole in turn increases the northward SST gradient in spring, while decreasing it in summer (see figure 2.b). This causes the wind anomalies to grow in spring, but to vanish in summer
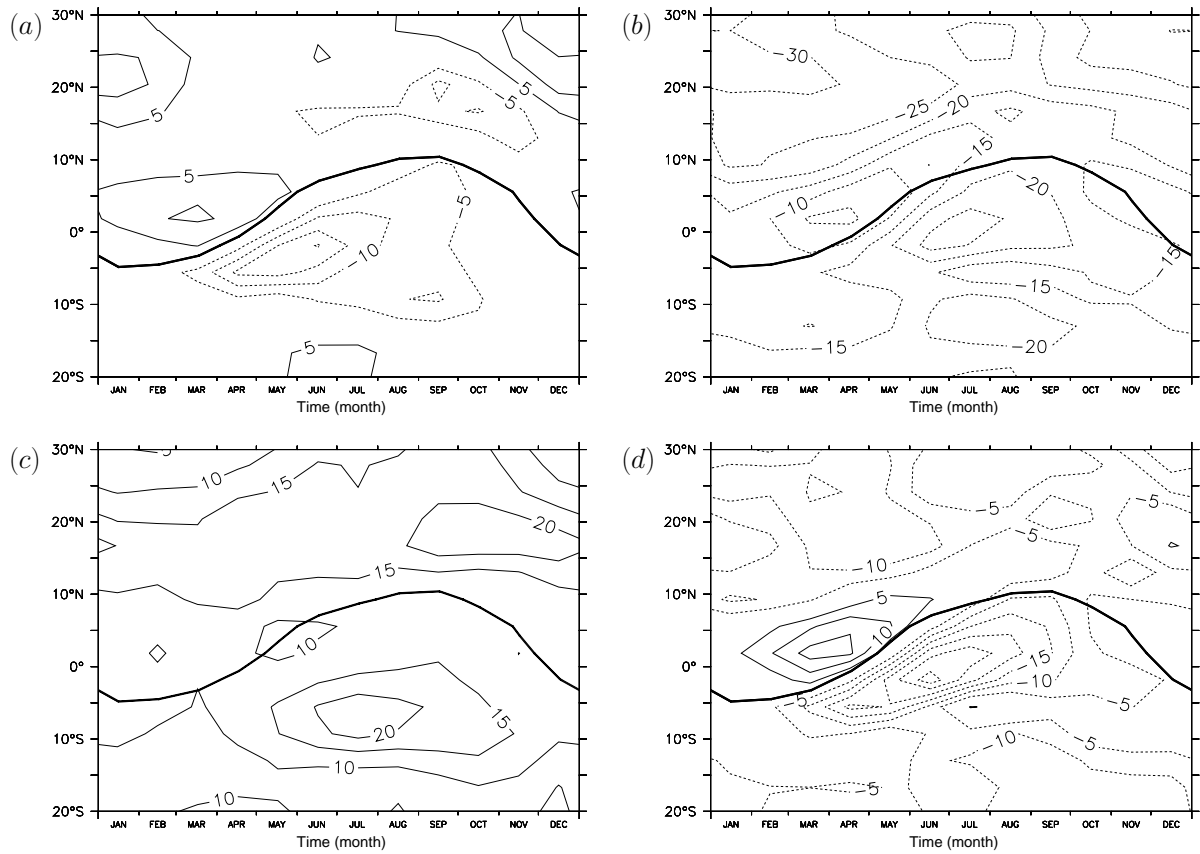
6

Figure 4: Relative contributions to changes in the downward latent heat flux shown in figure 3.a. (a) Wind-induced contribution ($\Delta\overline{LW}$). (b) Moisture-induced contribution ($\Delta\overline{LQ}$). (c) Stability-induced contribution ($\Delta\overline{LS}$). (d) Sum of (a)-(c).

and fall. Thus, figures 2-4 indicate indeed a positive WES feedback in spring, when the ITCZ is near the equator, but also a negative WES feedback in summer, when the ITCZ has moved towards the north of the deep NTA. Note that this mechanism may also partly explain why the shift in the ITCZ is largest in spring, while being smaller in summer and just marginal in fall.

Finally, we note that the changes in the climatological SSTs in case 2C are entirely due to changes in the net surface heat flux, because the ocean heat transport is prescribed and fixed in our simulations. Our model configuration lacks any dynamical response of the ocean to changes in the surface wind stress. To assess how the absence of a dynamical ocean response has affected the results, the changes in horizontal and vertical Ekman transport have been diagnosed (not shown). The C-shaped change in the surface wind stress field would cause a dipole pattern in vertical Ekman transport, with stronger upwelling south and weaker upwelling north of the equator. Furthermore, changes in horizontal Ekman transport would cause a positive heating tendency in the deep tropics from December till March, but a negative heating tendency during the rest of the year. This suggests that horizontal and vertical Ekman transport would act in concert to amplify the cross-equatorial SST gradient and thus the shift of the ITCZ from December till March, while they would impose opposite effects on the SST gradient and ITCZ position during the other months.

4 Changes in tropical Atlantic variability

4.1 Strength, structure and forcings of the meridional mode

To study the variability associated with the meridional mode, we use an NTA SST index defined as the spatial average of SST anomalies over the region spanning from 55-20°W and 5-25°N, which is similar to the definition used by Czaja et al. (2002). Figure 5 shows the standard deviation of this index as function of month. In accordance with observations, the standard deviation achieves its maximum in boreal spring, when the meridional mode is most dominant, and its minimum in boreal autumn. However, especially in boreal spring, the standard deviation of case 1C is too low by approximately 0.15 °C, which in part may be attributed to the absence of forcing by ENSO in our model simulations. Compared to case 1C, in case 2C the standard deviation has decreased by 0.04-0.05 °C or 10-20%, but the shape of the profile is similar, which is already an indication that there is no fundamental change in the underlying mechanisms of NTA variability.

Figure 6 gives an impression of the spatial structure of the meridional mode in boreal spring. It shows the regression of SST, near-surface wind, and net downward surface heat flux anomalies in April onto the normalized NTA SST index for boreal spring (i.e. the NTA SST index averaged over March-May and normalized such that its mean equals zero and its standard deviation equals unity). The general characteristics of the regressions patterns are similar for both cases, exhibiting anomalous surface heating in the southern NTA and a C-shaped anomalous wind pattern directed towards the positive SST anomalies. Different from case 1C, in case 2C the highest SST anomalies extend less far to the south west and the heat flux and wind anomalies in the southern NTA are considerably weaker.

The weaker anomalies in the southern NTA suggest that the WES feedback is less strong in case 2C. To further explore this, figure 7.a depicts the cross-correlation of an index for the southern NTA SSTs and an index for the cross-equatorial winds. These indices are defined as respectively the monthly SSTs averaged over 55-20°W and 5-15°N and the monthly meridional winds averaged over 50-20°W and 4°S-4°N. The cross-correlation for both case 1C and 2C is fairly symmetric around zero lag, which is indicative for a positive WES feedback and mutual reinforcement of SST and cross-equatorial wind anomalies (Von Storch and Zwiers 1999, Chang et al. 2001). In case 2C the maximum correlation is just slightly weaker, while the correlation
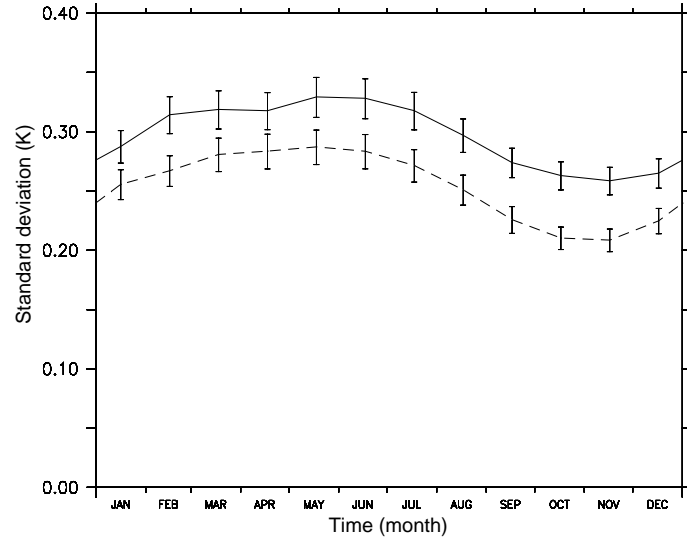
8

Figure 5: Standard deviation of the NTA SST index as function of month for case 1C (solid line) and case 2C (dashed line). Changes in standard deviation are significant at the 10 % level based on a two-tailed F-test (Von Storch and Zwiers 1999) for all months except April. Error bars show the standard deviations of the standard deviation estimate itself.
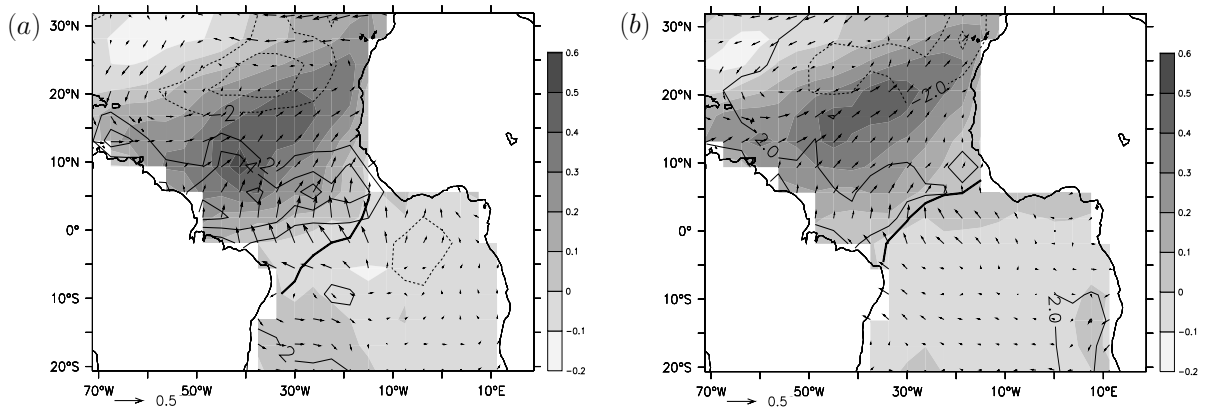

Figure 6: Regression of SST (colors, in °C), near-surface wind (vectors, in m/s) and downward net heat flux anomalies (thin contours, in W/m^2) in April onto the normalized NTA SST index for boreal spring (MAM), along with the cITCZ (thick line) for April. (a) Case 1C. (b) Case 2C.
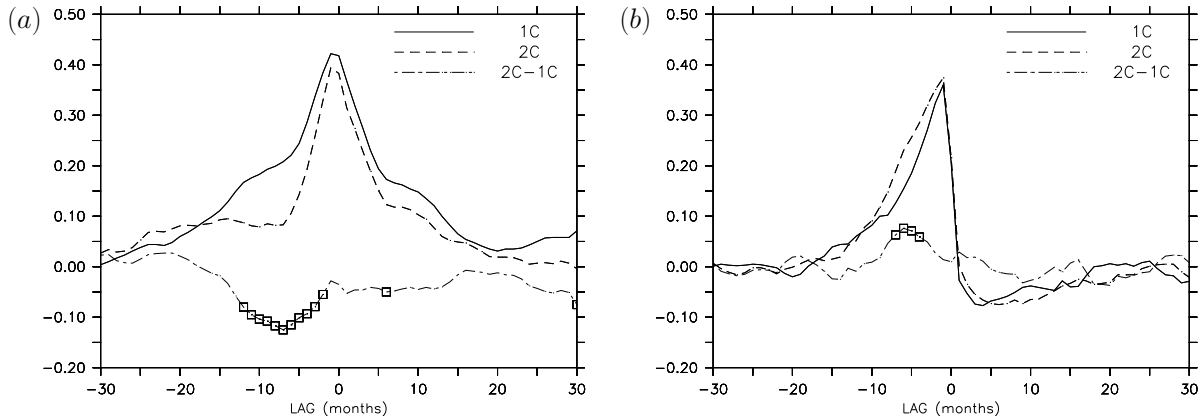
9

Figure 7: (a) Cross-correlation of southern NTA SST index (SSTs averaged over 55-20°W and 5-15°N) and cross-equatorial wind index (meridional winds averaged over 50-20°W and 4°S-4°N). SSTs lead cross-equatorial winds for positive lag. (b) Cross-correlation of northern NTA SST index and trade wind index (averages of respectively SSTs and zonal winds over 55-20°W and 15-25°N). SSTs lead winds for positive lag. The symbols indicate which correlation differences are significant at the 5 % level as calculated with help of the bootstrap method (Efron and Tibshirani 1998).

is confined to smaller lags, suggesting that the WES feedback is indeed weaker in case 2C.

When using the NTA SST index instead of the *southern* NTA SST index, the correlations in figure 7.a are less symmetric and have a smaller maximum value, which suggests that a positive WES feedback acts primarily in the deep tropics. To investigate this further, figure 7.b shows the cross-correlation between an index for the northern NTA SSTs and an index for the trade winds, defined as respectively the monthly SSTs and the monthly zonal winds averaged over 55-20°W and 15-25°N. In both case 1C and 2C the maximum correlation is found when the trade winds lead the SSTs by one month. The cross-correlation is clearly asymmetric around zero lag, which indicates that in the northern NTA the atmosphere is mainly forcing the ocean rather than the opposite (Von Storch and Zwiers 1999) and it confirms that a positive WES feedback is confined to the deep NTA, in accordance with earlier studies mentioned in the introduction section (e.g. Chang et al. 2000). Correlations for negative lags are somewhat higher in case 2C than in case 1C, which suggests that the forcing of the meridional mode by trade wind anomalies has become more important.

4.2   Onset, development and cessation of the meridional mode

In order to study the onset, development and cessation of the meridional mode, multiple lagged regressions of SST, near-surface wind and net heat flux anomalies onto the normalized NTA SST index for boreal spring (MAM) have been calculated and subsequently zonally averaged over the Atlantic from 55-20°W. Note from figure 6 that the anomalies are well represented by their zonal averages as their zonal variation is relatively small. Figure 8 depicts the zonally averaged lagged regressions in a time-latitude map, along with the zonally averaged climatological marine ITCZ (hereafter cITCZ for short). For comparison with observations, also the results are shown for the NCEP/NCAR reanalysis (Kalnay et al. 1996) of the period 1949-2003 (figure 8.a and calculated before by Czaja et al. 2002, their figure 2). To some extent the evolution of the meridional mode in observations has also been analyzed before by Chiang et al. (2002), although their composite analysis was based on an interhemispheric SST gradient index with the aim to study ITCZ variability. Houghton and Tourre (1992) showed that the SST anomalies over the

10

northern tropical Atlantic are only weakly anti-correlated with the SST anomalies over the southern tropical Atlantic, and the results of Chiang et al. (2002) therefore differ from Czaja et al. (2002).

Figure 9 presents the most dominant and spatially well-organized contributions to the net surface heat flux anomalies, which are the contributions from latent cooling and solar radiation. Similar as before in section 3, the latent heat flux anomalies have been decomposed into separate contributions from wind speed and specific humidity anomalies according to respectively:

$$LW = -L_v\overline{\rho_a C}\,\overline{(q_s - q)} \left(\sqrt{u^2 + v^2 + w_*^2}\right)' \tag{6}$$

$$LQ = -L_v\overline{\rho_a C}\,(q_s - q)'\,\overline{\sqrt{u^2 + v^2 + w_*^2}} \tag{7}$$

where the overbar denotes the climatological monthly mean and the prime the deviation from this mean. We verified that the sum of LW and LQ is close to the total latent cooling anomaly. The contribution from changes in the static stability parameter C appeared to be negligible. A similar decomposition of latent heat flux anomalies into a wind-induced part and a moisture-induced part has been made before by Saravanan & Chang (2000) and Chang et al. (2000).

4.2.1 Current climate

Below first the development of the meridional mode in case 1C is discussed. Thereafter the results are compared against the observations, and the implications of model biases are addressed.

North of 15°N the wind anomalies are predominantly zonal, whereas between 5°S-10°N they are mostly meridional. In the following we treat these regions separately. North of 15°N anomalous westerlies develop in November, which last until December between 25-30°N and until April near 15°N. The associated weakening of the northeasterly trade winds causes a reduction in wind-induced latent cooling (figure 9.a), and consequently positive SST anomalies start to grow. The SST anomalies reach their maximum roughly a month before the anomalous westerlies vanish and reverse sign, and then they gradually diminish in the following months as a result of moisture-induced and wind-induced latent cooling (see figures 9.a,b).

Between 0-10°N anomalous southerlies exist over the whole time range shown, displacing the ITCZ towards the north. They intensify when the SST anomalies start to grow and become strongest in May-July when the anomalous meridional SST gradient reaches a maximum. This supports the hypothesis that in the deep tropics a positive WES feedback takes place. The net surface heat flux anomalies in the region of 5°S-10°N prove to be closely related to the seasonal cycle of the cITCZ, being positive north of the cITCZ and negative south of the cITCZ. In part this can be explained by the sign change of the wind speed anomalies and consequently of the wind-induced latent heat flux (figure 9.a): in boreal winter and spring the anomalous southerlies act against the mean winds and therefore reduce the wind speed, whereas in summer and fall the southerlies point in the same direction as the mean winds and hence increase the wind speed. Thus, the positive WES feedback in winter and spring becomes a negative feedback in summer and fall. Supporting evidence for this comes also from the simulations of Chang et al. (2000, cf. their figures 10.e-g). It is also important that in the deep tropics moisture-induced latent cooling is negligible in boreal winter and spring, but strong in summer and fall (figure 9.b). Based on equation (7) this implies that in winter and spring $q' \approx q_s'$ and that in summer and fall $q' < q_s'$. Furthermore, because the saturation specific humidity is a function of SST alone according to the Clausius-Clapeyron equation, and the SST anomalies are not much stronger in the summer-fall period than in the winter-spring period, this suggests that the seasonality of LQ originates mainly from the anomalies in the near-surface specific humidity (q'). It is not the scope of the present paper to investigate this in more detail, but we speculate that the seasonality of q' is related to a change in anomalous moisture transport between the winter-spring and summer-fall
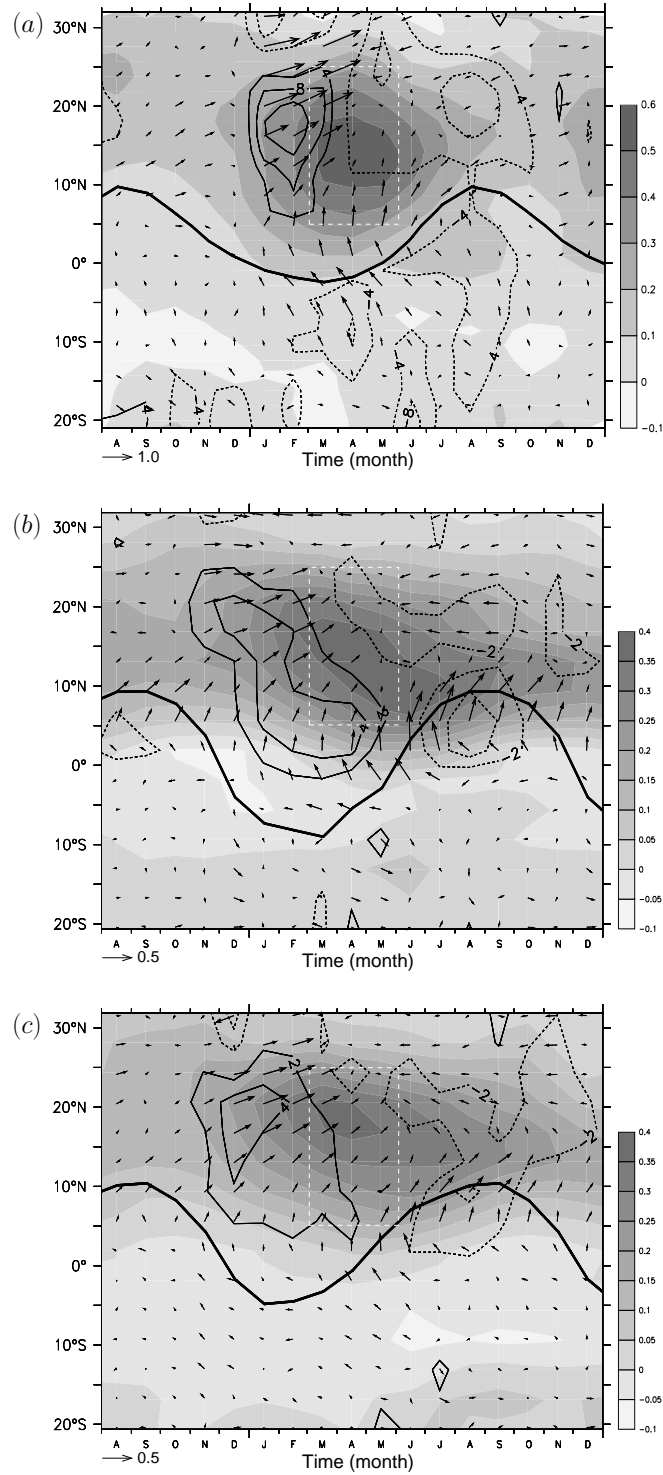
11

Figure 8: Time-latitude map of lagged regressions of SST (colors), near-surface wind (vectors) and net downward surface heat flux anomalies (thin contours) onto the normalized NTA SST index for boreal spring (indicated by the rectangle), all zonally averaged over the Atlantic from 55-20°W. The months prior to April correspond to negative lags, and the months after April to positive lags. The thick black line represents the location of the zonally averaged cITCZ. Units are the same as in figure 6. (a) NCEP/NCAR reanalysis. (b) Case 1C. (c) Case 2C. Note the difference in scaling between graph (a) and graphs (b),(c).
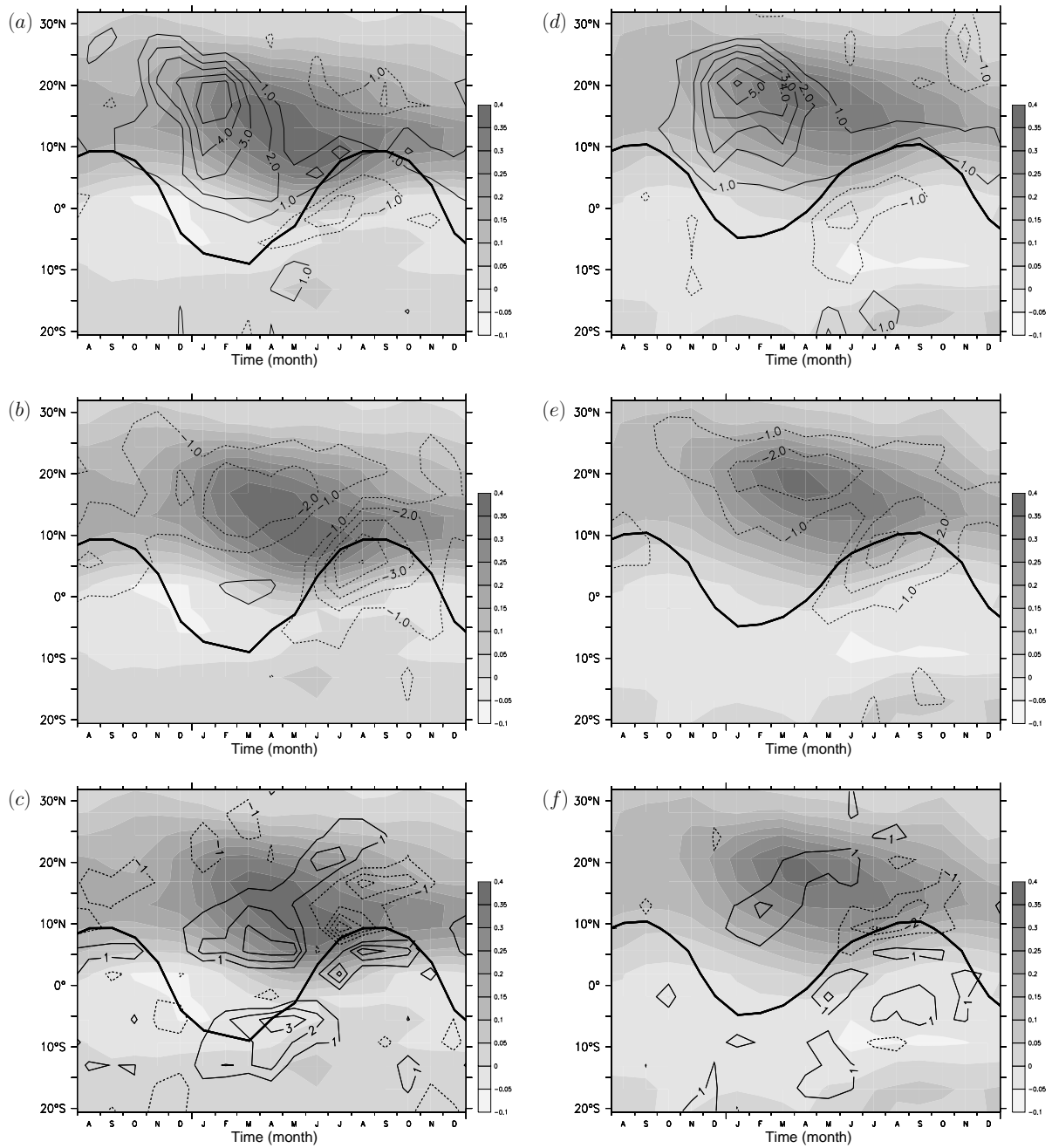
Figure 9: Same as in figure 8, but the thin contours now show the dominant terms in the ocean heat budget and the wind vectors have been omitted. Left panels correspond to case 1C, right panels to case 2C. (a),(d) Wind-induced latent heat flux anomalies (LW). (b),(e) Moisture-induced latent heat flux anomalies (LQ). (c),(f) Short-wave radiation anomalies (SW).

13

periods. In winter and spring, when the cITCZ is located south of the SST anomalies in the deep NTA, reduced entrainment of dry air from above into the convective boundary layer and moisture transport by both the mean and anomalous winds result in anomalous moistening of the convective boundary layer in the deep NTA, whereas the opposite holds for summer and fall. Figures 9.a,b show that in the deep tropics the WES feedback and the associated moisture transport act together to amplify the SST anomalies in winter and spring, and to damp the SST anomalies in summer and fall. A similar behavior is also observed in the simulations of Chang et al. (2000, cf. their figures 7.d,f) and Saravanan & Chang (2000).

Figure 9.c shows that short-wave radiation anomalies play a role in the deep NTA, although they are not the most dominant contribution to the net heat flux anomalies. The anomaly pattern is qualitatively consistent with the results of Frankignoul and Kestenare (2005) based on the NCEP/NCAR reanalysis (Kalnay et al. 1996). The positive radiation anomalies between 0-15°N in boreal winter and spring, when the cITCZ is located south of the deep NTA, are related to a positive feedback between low-level stratus cloud cover and SST (Okumura et al. 2001, Tanimito and Xie 2002, Klein and Hartmann 1993). The positive SST anomaly reduces the static stability on top of the boundary layer and as a result stratus cloudiness is reduced, which in turn via enhanced short-wave radiation reinforces the original SST anomaly. In summer and fall the cITCZ moves towards the north of the equator and consequently shifts over the SST anomaly in the deep NTA. The dipole short-wave radiation anomaly centered around the cITCZ in these seasons is related to a negative feedback between deep cumulonimbus clouds and SST (Okumura et al. 2001, Tanimito and Xie 2002). The anomalous southerly winds induced by the anomalous northward SST gradient displace the ITCZ towards the north (Chiang et al. 2002), causing an increase (decrease) in cumulonimbus cloudiness and hence a decrease (increase) in short-wave radiation north (south) of the cITCZ.

The development of the meridional mode in case 1C displays the salient features of its development in the observations (cf. figures 8.a,b). In both case 1C and the observations the meridional mode is triggered by wintertime trade wind anomalies and both indicate the existence of a positive WES feedback in the deep tropics in winter and spring. There are, however, also some notable differences between case 1C and the observations. The amplitude of the anomalies in the observations is generally stronger, which in part can be related to the absence of ENSO forcing in our model simulations. Furthermore, different from the observations, in case 1C the SST and heat flux anomalies appear to migrate towards the south by roughly 2°/month. This may originate from the absence of anomalous ocean heat transport by the mean meridional current in our simulations, which provides a negative feedback on SST anomalies in the southern NTA and tend to cancel the equatorward propagation of surface heat flux anomalies by a positive WES feedback (Xie 1999, Seager et al. 2001, Chang et al. 2001). This lack of damping by the ocean seems responsible for the persistence of SST and wind anomalies south of the cITCZ in summer and fall in case 1C, while in the observations the anomalies have then already been substantially damped. This may also explain that a negative WES feedback in summer and fall is more apparent in case 1C than in the observations. In the observations the negative surface heat flux and diminishing northward SST gradient and surface winds south of the cITCZ still hint on a negative WES feedback in summer and fall, but it seems of minor importance for damping of the meridional mode.

4.2.2 Double-CO_2 climate

Figures 8.b,c show that the general characteristics of the meridional mode are similar for case 1C and 2C. This suggests that there is no fundamental change in the mechanisms that generate the meridional mode. As in case 1C, positive SST anomalies start to grow in November. Averaged over 15-25°N and December-April, the anomalous westerlies and the associated reduction in

wind-induced latent cooling (cf. figures 9.a,d) are both more than 25 % stronger. Between 0-10°N the SST, meridional wind, and surface heat flux anomalies are significantly weaker. In the same region the wind-induced latent cooling and short-wave radiation anomalies are weaker in boreal winter and spring, which indicates that the positive WES and stratus-SST feedbacks are less strong in case 2C than in case 1C. This explains the reduced standard deviation of the NTA SST index depicted in figure 5. It also explains that the SST anomaly pattern is less tilted than in case 1C, as the positive feedbacks in the deep NTA are responsible for equatorward propagation of SST anomalies. Because the SST and wind anomalies in the deep tropics are weaker, also the damping by moisture-induced latent cooling in summer and autumn is reduced (cf. figures 9.b,e). Furthermore, because the wind anomalies in the deep tropical Atlantic are weaker, also the interannual variations in the position of the ITCZ are less strong.

In the next section we argue that the weaker WES feedback in the deep NTA originates from the northward displacement of the cITCZ.

5 Discussion

The results have shown that the meridional mode is weaker in case 2C, but that its mechanisms are not fundamentally different from case 1C. Figure 10 summarizes schematically the onset and development of the meridional mode in boreal winter and spring (a) and its cessation in the summer and fall (b). The acronyms represent the most important and spatially coherent terms in the ocean heat budget, which are: wind-induced latent heat flux (LW), moisture-induced latent heat flux (LQ) and short-wave radiation (SW) anomalies.

The trade wind anomalies that initiate growth of the meridional mode in boreal winter, are stronger in case 2C. Consequently, the positive wind-induced latent heat flux anomalies (LW) in the northern NTA have become stronger. In contrast with this, the positive wind-induced latent heat flux and short-wave radiation anomalies in the southern NTA have become weaker, indicating that the positive WES and stratus-SST feedbacks in boreal winter and spring are weaker. Consistent with the weaker feedbacks in the southern NTA, the SST anomalies in the northern NTA propagate less far towards the south. Because the SST anomalies in the southern NTA become not as strong as in case 1C, damping by moisture-induced latent cooling (LQ) in boreal summer and fall is also weaker. Furthermore, because the cross-equatorial wind anomalies are weaker, interannual variability in the location of the ITCZ is weaker, and hence the cumulonimbus-SST feedback is weaker (see the SW dipole in figure 10.b).

The present study confirms the conclusion in earlier studies, mentioned in the introduction, that the WES feedback is confined to the deep tropics. Czaja et al. (2002) and Saravanan & Chang (2004) suggested that this may be related to the increase of damping with climatological wind speed, see equation (7), which causes too much damping outside the deep tropics. In addition to this, wind speed anomalies create larger anomalies in wind-induced latent cooling in regions with larger climatological specific humidity difference, see equation (6), which also favors confinement of the WES feedback to the deep tropics.

In case 2C the cITCZ has shifted towards the north in boreal winter and spring, and one may expect that this is accompanied by a northward shift of the region in which a positive WES feedback could manifest itself. However, figure 2.b shows that changes in the climatological wind speed in case 2C are mostly confined to the deep tropics and in view of the discussion in the previous paragraph this suggests that the WES feedback remains confined to the deep tropics. Figures 7, 8 and 9 seem also not to indicate a shift of the WES region.

The results show that the WES feedback in the deep NTA exhibits phase-locking with the seasonal cycle of the cITCZ. This is schematically illustrated in figure 11. It shows that the wind anomaly in the deep NTA is directed against the mean wind when the cITCZ is at its southernmost position, near the equator, but points in the same direction when the cITCZ is
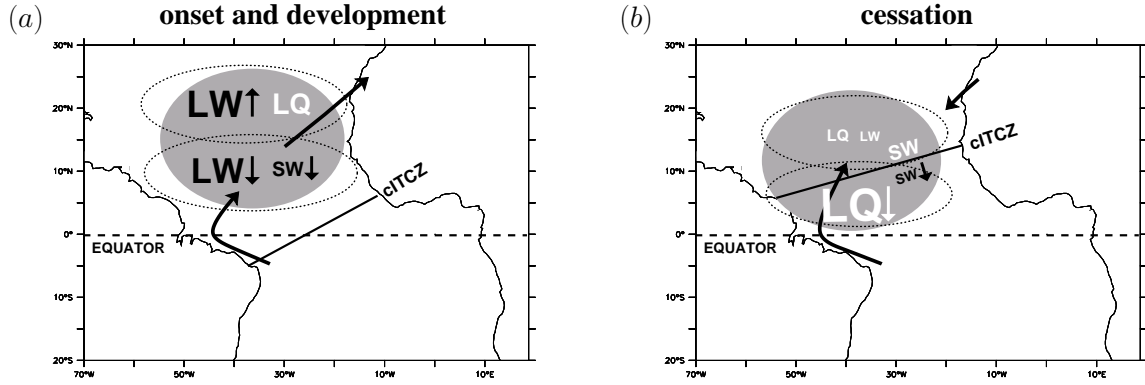
15

Figure 10: Schematic of the onset and development of the meridional mode in boreal winter and spring (a) and its cessation in summer and fall (b). The gray area represents a positive SST anomaly and the vectors the anomalies in near-surface winds. In each latitude band the most dominant and spatially coherent flux terms in the ocean heat budget are shown. The acronyms LW, LQ and SW denote respectively the wind-induced latent heat flux, the moisture-induced latent heat flux and short-wave radiation anomalies. The bigger an acronym, the larger the respective flux. The color black is used for positive SST tendencies, and white for negative tendencies. The relative changes in the fluxes in case 2C are indicated by the arrows behind the acronyms. Downward arrows are used for weaker fluxes, upward arrows for stronger fluxes, and no arrow behind an acronym means that the change is small.

at its northernmost position, near 10°N. The absolute wind speed is decreased in the first case, while it is enhanced in the second case, resulting in weaker (positive WES) and stronger cooling (negative WES), respectively. In the deep NTA also moisture-induced latent cooling is subject to phase-locking with the seasonal cycle of the cITCZ. Anomalous moisture transport attenuates damping of the SST anomalies when the cITCZ is at its southernmost position, but reinforces damping when the cITCZ is at its northernmost position.

From the above reasoning it follows that the longer the cITCZ stays near the equator, or more specific south of the deep NTA, the longer a positive WES feedback may amplify the SST anomaly before damping by moisture-induced latent cooling and (to less extent) a negative WES feedback becomes active. A similar conclusion about the relation between the strength of the WES feedback and the cITCZ is drawn in the study of Okajima et al. (2003). The shorter period that the cITCZ stays south of the deep NTA in case 2C may thus explain the overall weaker WES feedback in the deep NTA (cf. figures 8.b,c). We note furthermore that because the SST anomalies in the deep NTA are smaller owing to the weaker WES feedback, this may in fact also explain the weaker stratus-SST feedback.

The relation between the weaker WES feedback in the deep NTA and the northward shift of the cITCZ prompts the question about the origin of the shift in the cITCZ. The results presented in section 3 indicate that the northward shift of the cITCZ in boreal winter and spring is related to a change in the northward SST gradient, and that it can be largely explained by means of positive WES feedback. Just as we have seen before for the seasonal cycle of the meridional mode, the WES feedback acting on the cITCZ is positive in boreal spring, but negative in summer and fall, related to the position of the cITCZ with respect to the deep NTA. Furthermore, the results indicate that the changes in the winds are accompanied by changes in moisture transport, which tend to attenuate latent cooling in spring, while enhancing it in summer. The change in the WES feedback and associated moisture transport from spring to summer may explain that

the shift in the cITCZ is most pronounced in spring, while it is small in summer and fall. This implies that the anthropogenic change of the cITCZ is subject to phase-locking with the seasonal cycle of the cITCZ itself. Another factor that may have played a role for the asymmetric shift in the cITCZ is that the interhemispheric SST gradient is relatively weak in spring compared to summer, which makes the cITCZ more susceptible to small changes in the SST gradient in spring than in summer and fall (Chiang et al. 2002).

The fact that a positive WES feedback in the deep NTA is responsible for the northward shift of the cITCZ, does not yet explain why the changes in the mean SSTs are stronger north than south of the cITCZ, and how this can be related to the change in the atmospheric CO_2 concentration. However, just as for case 2C, climate projections from coupled GCMs for the twenty-first century also exhibit stronger warming of the northern than the southern hemisphere, especially at the high northern latitudes, although less strong over the North Atlantic related to a slowdown of the meridional overturning circulation (IPCC 2001). Studies by Chiang and Bitz (2005) and Broccoli et al. (2006) suggest that an interhemispheric asymmetry in warming at high latitudes will shift the cITCZ towards the warmer hemisphere, a hypothesis supported by recent paleoclimatic evidence (e.g. Peterson et al. 2000, Wang et al. 2004) and consistent with the northward shift of the cITCZ in case 2C.

We briefly discuss the main restrictions of our study. Inherent to the use of a passive mixed-layer model for the ocean, the ENSO forcing of the meridional mode has not been simulated. The teleconnection with the NAO has also not been discussed in this paper, as unfortunately in our simulations the southern lobe of the NAO does not extend far enough into the tropics and consequently the impact of the NAO on the meridional mode is small. However, the wintertime trade wind anomalies that force the meridional mode are still accompanied by variations in the subtropical high, as can be expected based on geostrophic balance. Regression of wintertime mean-sea-level pressure anomalies onto the MAM NTA SST index revealed a pressure tripole pattern over the northern Atlantic with its most southern and relatively weak lobe in the sub-tropics (not shown). This pattern does not project well on the dipole pattern of the NAO, but similar to the NAO it is of stochastic nature. Because the subtropical forcing of the meridional mode is fairly similar both in the observations as in our model runs, this seems to indicate that the forcing originates not so much from the NAO, but rather from stochastic variation in the subtropical high (which in the observations projects on the NAO). Support for this comes from the study of Czaja et al. (2002), who successfully hindcasted the NTA SST time series by means of a simple model in which the external forcing is represented by pressure variations of the subtropical high.

Because the ENSO and NAO forcings are not (well) simulated by our model, it remains uncertain how the external forcing of the meridional mode will change. We note that also future climate projections from coupled GCMs disagree on changes in strength and preferred frequencies of ENSO and the NAO (IPCC 2001).

Another restriction of this study is that the ocean heat transport has been prescribed and fixed in our simulations. At the end of section 3 we already discussed how the lack of adjustment in ocean Ekman transport has affected our results. Our ocean model also lacks adjustment in the thermohaline circulation, which most coupled GCMs show to weaken. Studies by Dong and Sutton (2002) and Zhang and Delworth (2005) indicate that a weakening of the thermohaline circulation tend to cool the North Atlantic, while warming the South Atlantic, along with a southward shift of the cITCZ in the tropical Atlantic. However, as we mentioned earlier in this section, most future climate projections from coupled GCMs show still a stronger warming of the northern hemisphere due to the overwhelming effect of radiative forcing by the increase in greenhouse gases, which suggests that the cITCZ will shift towards the north.
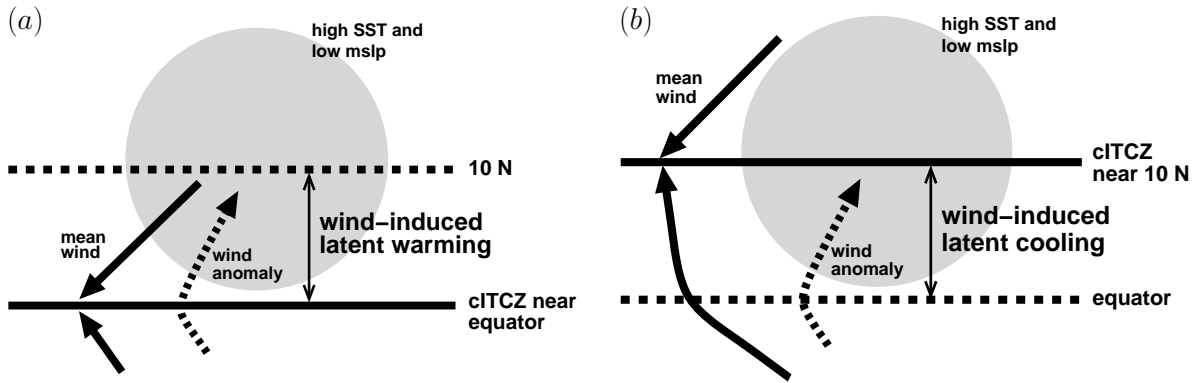
Figure 11: Phase-locking of the WES feedback in the deep NTA (roughly between 0-10°N) with the seasonal cycle of the cITCZ. The WES feedback is positive when the cITCZ is located close to the equator (a), and negative when it is located north of the deep NTA region (b).

6   Summary and conclusions

The influence of a doubling of atmospheric CO_2 on the meridional mode in the NTA has been studied. The numerical model consists of an atmospheric GCM of intermediate complexity compared to present state-of-the-art models and a passive mixed-layer model for the ocean with prescribed climatological ocean heat transport. Results from two runs have been shown: a control run with present-day atmospheric CO_2, and a run with a doubled atmospheric CO_2 concentration. The control run captures the characteristic features of the meridional mode reasonably well. The main difference from observations is the absence of ENSO forcing of the subtropical trade wind anomalies in boreal winter and spring, which is implicit to the nature of our ocean model.

The meridional mode is initiated in boreal winter by stochastic forcing of trade wind anomalies, which persists roughly till boreal spring. These trade wind anomalies are responsible for a reduction in wind-induced latent cooling in the northern NTA, which in turn causes growth of SST anomalies. In the deep NTA a positive WES feedback exists during boreal winter and spring, which causes equatorward propagation of the surface heat flux and SST anomalies. There is evidence of a positive stratus-SST feedback in the deep NTA in boreal winter and spring and a negative cumulonimbus-SST feedback near the cITCZ in summer and fall, although they are not of primary importance for the evolution of the meridional mode. The cessation of the meridional mode takes place in boreal summer and fall, when damping by moisture-induced latent cooling becomes dominant, especially in the deep NTA.

The results from the double-CO_2 run show a pronounced northward shift of the cITCZ in the tropical Atlantic in boreal winter and especially in spring, when it amounts roughly 5° averaged over 55-20°W, but just a marginal shift in summer and fall. The meridional mode weakens in the double-CO_2 run, but its structure and underlying mechanisms have not fundamentally changed. The strength of the meridional mode, as characterized by the NTA SST index, is reduced by 0.04-0.05 °C or 10-20 % throughout the seasons.

The northward shift in the cITCZ in boreal winter and spring can be related to an increase in the northward SST gradient near the equator and a positive WES feedback acting in the deep tropical Atlantic. The marginal shift in the cITCZ in boreal summer and fall seems to originate from the sign change in the WES feedback and associated moisture transport when the cITCZ moves from the equator towards the north of the deep NTA. The anthropogenic change of the cITCZ is thus subject to phase-locking with the seasonal cycle of the cITCZ itself.

In the double-CO_2 run the weakening of the positive WES feedback and to less extent the stratus-SST feedback in the deep NTA during boreal winter and spring is stronger than the enhanced external forcing by the trade wind anomalies in the northern NTA during the same seasons. The weaker positive WES feedback is attributed to the northward shift of the cITCZ in boreal winter and spring. This shift has resulted in a shortening of the time period during which the cITCZ stays south of the deep NTA. As a consequence, the positive WES feedback in the deep NTA acts less long and the damping of the meridional mode by moisture-induced latent cooling starts earlier as compared to the control run.

From our study two important implications can be drawn for future climate change. The first is that changes in the location of the cITCZ will likely be strongest in boreal spring when the cITCZ is nearest to the equator as in that case it is most susceptible to a positive WES feedback in the deep tropical Atlantic. It may be expected that the cITCZ will shift towards the north in boreal spring if warming of the northern hemisphere is indeed stronger than of the southern hemisphere, but will shift to the south in the opposite case. The second implication is that changes in the position of the cITCZ will change the strength of the WES feedback acting on variability in the deep tropical Atlantic. The WES feedback weakens when the cITCZ shifts towards the north, but strengthens when the cITCZ shifts towards the south.

Finally we note that changes in the position of the cITCZ and the strength of the WES feedback will have consequences for the amount and variation of rainfall in the neighboring continents. For instance, the expected northward shift of the cITCZ and its associated rainfall will reduce mean rainfall over the semi-arid region of northeastern Brazil, but will increase it further to the north of South-America, while a simultaneous weakening of the WES feedback reduces meridional excursions of the cITCZ and hence tend to reduce interannual variations in rainfall.

7   References

Biasutti, M., A. H. Sobel, and Y. Kushnir (2006) AGCM precipitation biases in the tropical Atlantic. *J. Clim.,* **19**, 935–958.

Carton, J. A., X. Cao, B. J. Giese, and A. M. da Silva (1996) Decadal and interannual SST variability in the tropical Atlantic ocean. *J. Phys. Oceanogr.,* **26**, 1165-1175.

Chang, P., L. Ji, and H. Li (1997) A decadal climate variation in the tropical Atlantic ocean from thermodynamic air-sea interactions. *Nature,* **385**, 516-518.

Chang, P., R. Saravanan, L. Ji, and G. C. Hegerl (2000) The effect of local sea surface temperatures on atmospheric circulation over the tropical Atlantic sector. *J. Clim.,* **13**, 2195-2216.

Chang, P., L. Ji, and R. Saravanan (2001) A hybrid coupled model study of tropical Atlantic variability. *J. Clim.,* **14**, 361-390.

Chiang, J. C. H., and C. M. Bitz (2005) Influence of high latitude ice cover on the marine Intertropical Convergence Zone. *Climate Dynamics,* **25**, 477-496.

Czaja, A., P. van der Vaart, and J. Marshall (2002) A diagnostic study of the role of remote forcing in Tropical Atlantic variability, *J. Clim.,* **15**, 3280-3290.

Czaja, A. (2004) Why is north tropical Atlantic SST variability stronger in boreal spring? *J. Clim.,* **17**, 3017-3025.

Dong, B.-W., and R. T. Sutton (2002) Adjustment of the coupled ocean-atmosphere system to a sudden change in the Thermohaline Circulation. *Geophys. Res. Lett.,* **29**, 1728.

Efron, B., and R. J. Tibshirani (1998) An introduction to the bootstrap. Chapman and Hall.

Folland, C. K., T. N. Palmer, and D. E. Parker (1986) Sahel rainfall and worldwide sea temperatures. *Nature,* **320**, 602-607.

Frankignoul, C., and E. Kestenare (2005) Air-sea interactions in the tropical Atlantic: a view based on lagged rotated maximum covariance analysis. *J. Climate,* **18**, 3874-3890.

Haarsma, R. J., E. J. D. Campos, W. Hazeleger, C. Severijns, A. R. Piola, and F. Molteni (2005) Dominant modes of variability in the south Atlantic: a study with a hierarchy of ocean–atmosphere models. *J. Clim.,* **18**, 1719-1735.

Hastenrath, S. (1984) Interannual variability and annual cycle: Mechanisms of circulation and climate in the tropical Atlantic. *Mon. Wea. Rev.,* **112**, 1097-1107.

Hazeleger, W., C. Severijns, R. Haarsma, F. Selten, and A. Sterl (2003) SPEEDO–Model description and validation of a flexible coupled model for climate studies, *Techn. Rep. TR-257,* R. Neth. Meteorol. Inst. (KNMI), De Bilt, Netherlands.

Hazeleger, W., C. Severijns, R. Seager, and F. Molteni (2005) Tropical Pacific-driven decadal energy transport variability. *J. Clim.,* **18**, 2037-2051.

Held, I. M., and B. J. Soden (2006) Robust responses of the hydrological cycle to global warming. *J. Clim.,* to appear.

Houghton, R. W., and Y. M. Tourre (1992) Characteristics of low-frequency sea surface temperature fluctuations in the tropical Atlantic. *J. Clim.,* **5**, 765-771.

IPCC (2001) Climate change 2001: The scientific basis. Contribution of Working Group I to the Third Assessment Report of the IPCC. Cambridge University Press, Cambridge. (available at http://www.ipcc.ch)

Kalnay, E., M. Kanamitsu, R. Kistler, W. Collins, M. I. Deaven, L. Gandin, M. Iredell, S. Saha, G. White, J. Woollen, Y. Zhu, M. Chelliah, W. Ebisuzaki, W. Higgins, J. Janowiak, K.C. Mo, C. Ropelewski, A. Leetmaa, R. Reynolds, R. Jenne, and D. Joseph (1996) The NCEP/NCAR 40-year reanalysis project, *Bull. Amer. Meteorol. Soc.,* **77**, 437-471.

Klein, S. A., and D. L. Hartmann (1993) The seasonal cycle of low stratiform clouds. *J. Climate,* **6**, 1587-1606.

Kushnir, Y., R. Seager, and J. Miller (2002) A simple coupled model of tropical Atlantic decadal climate variability. *Geophys. Res. Lett.,* **29**, 2133.

Lindzen, R. S., and S. Nigam (1987) On the role of sea surface temperature gradients in forcing low-level winds and convergence in the tropics. *J. Atmos. Sci.,* **44**, 2418-2436.

Marshall, J., Y. Kushnir, D. Battisti, P. Chang, A. Czaja, R. Dickson, J. Hurrell, M. McCartney, R. Saravan, and M. Visbeck (2001) North Atlantic climate variability: phenomena, impacts and mechanisms. *Int. J. Climatol.,* **21**, 1863-1898.

Molteni, F. (2003) Atmospheric simulations using a GCM with simplified physical parameterizations. I: model climatology and variability in multi-decadal experiments. *Clim. Dyn.,* **20**, 175-191.

Moura, A. D., and J. Shukla (1981) On the dynamics of droughts in northeast Brazil: observations, theory and numerical experiments with a general circulation model. *J. Atmos. Sci.,* **38**, 2653-2675.

Nobre, P., and J. Shukla (1996) Variations of sea surface temperature, wind stress, and rainfall over the tropical Atlantic and South America. *J. Clim,* **9**, 2464-2479.

Okajima, H., X.-P. Xie and A. Numaguti (2003) Interhemispheric coherence of tropical climate variability: Effect of climatological ITCZ. *J. Meteor. Soc. Japan,* **81**, 1371-1386.

Okumura, Y., S.-P. Xie, A. Numaguti, and Y. Tanimoto (2001) Tropical Atlantic air-sea interaction and its influence on the NAO. *Geophysical Res. Let.,* **28**, 1507-1510.

Peterson, L.C., G. H. Haug, K. A. Hughen, and U. Rohl (2000) Rapid changes in the hydrologic cycle of the tropical Atlantic during the last glacial. *Science,* **290**, 1947-1951.

Ruiz-Barradas, A., J. A. Carton, and S. Nigam (2000) Structure of interannual-to-decadal climate variability in the tropical Atlantic sector. *J. Clim.,* **13**, 3285-3297.

Saravanan, R., and P. Chang (2000) Interaction between tropical Atlantic variability and El Niño-Southern Oscillation. *J. Clim.,* **13**, 2177-2194.

Seager, R., Y. Kushnir, P. Chang, N. Naik, J. Miller, and W. Hazeleger (2001) Looking for the role of the ocean in the Tropical Atlantic decadal climate variability, *J. Clim.,* **14**, 638-655.

Sutton, R.T., S. P. Jewson, and D. P. Rowell (2000) The elements of climate variability in the tropical Atlantic region. *J. Clim.,* **13**, 3261-3284.

Tanimoto, Y., and S.-P. Xie (2002) Inter-hemispheric decadal variations in SST, surface wind, heat flux and cloud cover over the Atlantic ocean. *J. Meteor. Soc. Japan,* **80**, 1199-1219.

Von Storch, H., and F. W. Zwiers (1999) Statistical analysis in climate research. Cambridge University Press, Cambridge.

Wang, X., A. S. Auler, R. L. Edwards, H. Cheng, P. S. Cristalli, P. L. Smart, D. A. Richards, and C.-C. Shen (2004) Wet periods in northeastern Brazil over the past 210 kyr linked to distant climate anomalies. *Nature,* **432**, 740-743.

Xie, S.P., and S. G. H. Philander (1994) A coupled ocean-atmosphere model of relevance to the ITCZ in the eastern Pacific. *Tellus,* **46A**, 340-350.

Xie, S.-P. (1999) A dynamic ocean-atmosphere model of the tropical Atlantic decadal variability. *J. Clim.,* **12**, 64-70.

Xie, S.-P., and J. A. Carton (2004) Tropical Atlantic variability: patterns, mechanisms, and impacts. In *Earth Climate: The Ocean-Atmosphere Interaction*, C. Wang, S.-P. Xie, and J.A. Carton (eds.), Geophysical Monograph, 147, AGU, Washington D.C., 121-142.

Zebiak, S. E. (1993) Air-sea interaction in the equatorial Atlantic region. *J. Clim.,* **6**, 1567-1586.